FEBS Letters 587 (2013) 2412–2419

FEBS Letters

journal homepage: www.FEBSLetters.org

The anti-inflammatory drug celecoxib inhibits t-type Ca^{2+} currents in spermatogenic cells yet it elicits the acrosome reaction in mature sperm

E. Balderas [a], C. Sánchez-Cárdenas [a], J.C. Chávez [a], J.L. de la Vega Beltrán [a], F. Gómez-Lagunas [b], C.L. Treviño [a], A. Darszon [a,*]

[a] Departamento de Genética del Desarrollo y Fisiología Molecular, Instituto de Biotecnología, Universidad Nacional Autónoma de México (UNAM), Avenida Universidad 2001, Col. Chamilpa, C.P. 62210 Cuernavaca Mor., Mexico

[b] Facultad de Medicina, Edificio de Investigación 1er piso, Universidad Nacional Autónoma de México (UNAM), Avenida Universidad 2001, Col. Chamilpa, C.P. 62210 Cuernavaca Mor., Mexico

ARTICLE INFO

Article history:
Received 26 February 2013
Revised 28 May 2013
Accepted 30 May 2013
Available online 13 June 2013

Edited by Maurice Montal

Keywords:
Celecoxib
T-type channel
Acrosome reaction
Anti-inflammatory drug
Fertilization

ABSTRACT

Celecoxib (Cx), an anti-inflammatory drug designed to inhibit COX2, can affect some ion channels. T-type (Ca_V3) channels have been implicated in sperm physiology. Here we report and characterize the Cx induced inhibition of T-type channels in mouse spermatogenic cells. Unexpectedly, Cx can also induce the acrosome reaction (AR), an intracellular Ca^{2+} ($[Ca^{2+}]_i$) increase and a sperm depolarization. This $[Ca^{2+}]_i$ increase possibly results from the ability Cx has to alkalinize intracellular pH (pH_i), which is known to activate the sperm specific Ca^{2+} channel CatSper. As the Cx induced $[Ca^{2+}]_i$ increase is sensitive to mibefradil, a CatSper blocker, this channel may mediate the Cx-induced Ca^{2+} entry leading to the AR. Our observations demonstrate that Cx can compromise fertilization.

1. Introduction

Celecoxib (Cx) is a non-steroidal anti-inflammatory drug (NSAID) designed to specifically inhibit the inflammation-induced cycloxygenase 2 (COX-2) over its constitutively expressed COX-1 enzyme isoform. Nonetheless, it has been found that at concentrations within the order reached in patient's plasma (5–15 μM) [31], in addition to this intended pharmacological target, Cx directly inhibits several ion channels ($IC_{50} \sim 0.5$–30 μM) [1,6,13,14,23,30,41].

The sperm acrosome reaction (AR) is an exocytotic event triggered, amongst other ligands, by the zona pellucida (ZP), the envelope that surrounds the egg. The AR is a process required for the sperm to fuse and fertilize the egg, and it involves an increase in the sperm intracellular Ca^{2+} concentration ($[Ca^{2+}]_i$) (reviewed in [11]). The Ca_V3 channel family has been proposed to participate in the AR [2,20] and its three members have been immunologically identified in sperm [11]. However, until now Ca^{2+} currents (I_{Ca}) due to low-voltage activated T-type $Ca_V3.2$, and possibly 3.1 isoforms have been recorded either in mouse spermatogenic cells [2–4,15,20,32,34] or in testicular sperm [25], but not in mature spermatozoa [22].

In addition to the proposed Ca_v channels, a sperm specific Ca^{2+}-permeable channel named CatSper has been recorded and shown to contribute to $[Ca^{2+}]_i$ elevation in mature mammalian sperm [7,18,21,33,37,40]. It turns out that the two known sperm specific channels required for fertilization, CatSper and SLO3, a K^+ channel are up-regulated by cytoplasmic alkalinization [11,18,22,25,27,39,40,42,43].

As Cx has been recently shown to exert an antagonist effect on L-type Ca^{2+} channels [36,41] and Shab K^+ channels [1], we decided to examine if it blocked the Ca_v3 channels in spermatogenic cells and affected mouse sperm physiology. We are interested in finding compounds that may affect the Ca^{2+} channels present in sperm, as tools to elucidate their contribution to cell physiology and fertilization.

Herein we report that at concentrations within the order reached in patient's plasma (5–15 μM), [31] Cx inhibit Ca_v3 (T-type Ca^{2+}) currents in pachytene spermatocytes (referred as spermato-

* Corresponding author. Fax: +52 777 3172388.
E-mail address: darszon@ibt.unam.mx (A. Darszon).

0014-5793/$36.00
http://dx.doi.org/10.1016/j.febslet.2013.05.068

genic cells in the rest of the text), an effect that may compromise the process of spermatogenesis in mammals [11]. Additionally, and unexpectedly, when found that Cx depolarizes the sperm membrane potential, and elevates both $[Ca^{2+}]_i$ and pH_i inducing the AR. Ultimately and importantly, these effects will prevent sperm from reaching the ovum and fertilizing it.

2. Methods

2.1. Isolation of spermatogenic cells

Cells were isolated from CD-1 adult mice (8–12 weeks old) bred following the approved guidelines of the local Animal Care and Bioethics committee, as previously reported [4].

2.2. Electrophysiological recordings

Macroscopic currents were recorded under whole-cell patch-clamp with an Axopatch 200A amplifier (Molecular Devices, Sunnyvale, CA). Signals were filtered at 2 kHz with the built-in filter of the amplifier, and digitized at 10 kHz using a Digidata 1200A interface (Molecular Devices, CA). The bath solution (BS) contained (in mM): 2 $CaCl_2$; 130 NaCl; 3 KCl; 2 $MgCl_2$; 1 $NaHCO_3$; 0.5 NaH_2PO_4; 5 HEPES; 10 glucose, pH 7. The internal solution consisted of (in mM): 120 $CsMeSO_3$; 10 CsF; 15 CsCl; 5 EGTA; 5 HEPES; 4 Mg-ATP; 10 phosphocreatine, pH 7.3. About 80% of the series resistance was compensated. Holding potential (HP) was −90 mV.

Celecoxib (4-[5-(methyl-phenyl)-3-(trifluoromethyl)-1*H*-pyrazol-1-yl] benzene-sulfonamide (Cx) was obtained from pharmacy capsules, as reported [13,14], and dissolved in DMSO (0.1% maximum) (Sigma–Aldrich, St. Louis, MO).

2.3. $[Ca^{2+}]_i$ measurements

Epididymal sperm were collected by swim-up in Whitten's medium supplemented with 2 mM Ca^{2+} at 37 °C. Cells were incubated with 2 μM Fluo-4 AM (Invitrogen, Life Technologies, NY) and 0.05% pluronic acid at 37 °C during 30 min. Once loaded, sperm were centrifuged to eliminate external dye and resuspended in Whitten's with or without 2 mM Ca^{2+}, depending on the experimental conditions. Thereafter, the sperm suspension was placed in a recording chamber and the cells immobilized on mouse laminin (2 mg/ml, Invitrogen, Life Technologies, NY) coated cover slips and the recording chamber was filled with the proper medium. In the blocking experiments mibefradil was added in the medium 5 min before starting the Ca^{2+} recordings. Fluo-4 was excited with stroboscopic LED-based fluorescence illumination system using a Fluo 4 filter set (Excitation D: 480/30; DCLP 505; Emission 535/40; Chroma Technology Corp.). Fluorescence was captured at 2 Hz with a Cool Snap ES CCD camera (Photometrics USA) and expressed as $F - F_0/F_0$ (F is probe Fluorescence and F_0 basal fluorescence), as previously described [28].

2.4. Intracellular pH (pH_i) measurements

pH_i was estimated as previously described [9]. Briefly, spermatozoa (4×10^6 cells/ml) were loaded with 0.5 μM of the fluorescent dye 2′,7′-bis-(2-carboxyethyl)-5-(and-6)-carboxyfluorescein (BCECF, Molecular Probes Eugene, OR, USA) 15 min at 37 °C prior the experiments. The pH calibration was performed as reported before [12]. BCECF ratio values were converted to pH_i with the software FeliX (Photon Technology International, Birmingham, NJ). The experiments were conducted on non-capacitated mice spermatozoa.

2.5. Acrosome reaction assays

Mouse sperm selected by swim-up [16] were capacitated during 40 min at 37 °C in Whitten's medium. Thereafter, AR was induced by adding 15 μM A-23187 (Sigma, St Louis MO) at 37 °C and compared with those cells exposed to Cx (5–200 μM). AR was determined in formaldehyde-fixed sperm as previously described [26].

2.6. Membrane potential measurements

Membrane potential was measured using 3,3′-dipropylthiocarbocyanine iodide ($DisC_3$ (5); Molecular Probes). Fluorescence was monitored with a Hansatech MkII fluorometer (Norfolk, UK) at 620/670 nm excitation/emission wavelength pair. Recordings were initiated after reaching steady-state fluorescence (1–3 min) and were converted to membrane potential as described previously [26].

3. Results

3.1. Cx inhibited T-type calcium currents in spermatogenic cells

As a first step to determine the influence of Cx on fertilization we tested its effect on T-type Ca^{2+} currents which are the predominant voltage-dependent conductance of mouse spermatogenic cells [11]. Fig. 1A illustrates control Ca^{2+} currents (I_{Ca}) recorded by activating the channels with 350-ms depolarizations from −80 to +50 mV, applied in 10 mV steps from a HP of -90 mV. I_{Ca} activates at ∼−60 mV, reaches its peak amplitude at ∼−25 mV, and presents the fast open-state inactivation characteristic of T-type currents. Once control I_{Ca} was recorded, the cell was extensively superfused with an external solution containing 50 μM Cx and the activity of the channels was tested. Fig. 1B shows that interestingly Cx inhibited ∼60% of I_{Ca} at all voltages. The latter is best seen in Fig. 1C which presents the normalized average *I–V* curves obtained from experiments as in A and B, as indicated.

In contrast to its effect on some K^+ channels where Cx speeds open state inactivation (e.g., see [1, 14]), the rate of I_{Ca} inactivation was not changed (not shown, but apparent in the traces). The effect of Cx is further characterized in Fig. 1D which displays the Cx dose–response curve obtained from experiments as in Fig. 1A and B (see figure legend). The line is the fit of the average points with a Hill equation with K_d of 27 μM and Hill number $n = 0.93$, suggesting that a single Cx molecule binds to each channel, inhibiting Ca^{2+} permeation (see below). It is important to point out that the measured K_d falls within the range of the reported values found for all the other ion channels tested so far (see Section 1).

3.2. Cx effects on the gating of T-type Ca^{+2}channels

Cx inhibition was further characterized by studying its effect on the steady-state activation and inactivation curves of T type Ca^{2+} channels. We used a standard two-pulse protocol to determine both curves (see top of Fig. 2A). Channel activation was determined by the chord conductance obtained measuring peak I_{Ca} evoked by 200-ms depolarizing pulses of a variable amplitude that activated and inactivated I_{Ca}. The inactivated state of the channels was determined by the current evoked by a second test-pulse of −20 mV, applied immediately after the long depolarizing pulses (see Fig. 2 legend). Fig. 2A and B are representative I_{Ca}s obtained with the above pulse protocol applied either with 0 (Control) or 50 μM Cx, respectively. The points in Fig. 2C show that Cx did not modify the voltage dependence of activation, demonstrating that I_{Ca} reduction in the presence of Cx is not due to a voltage shift of

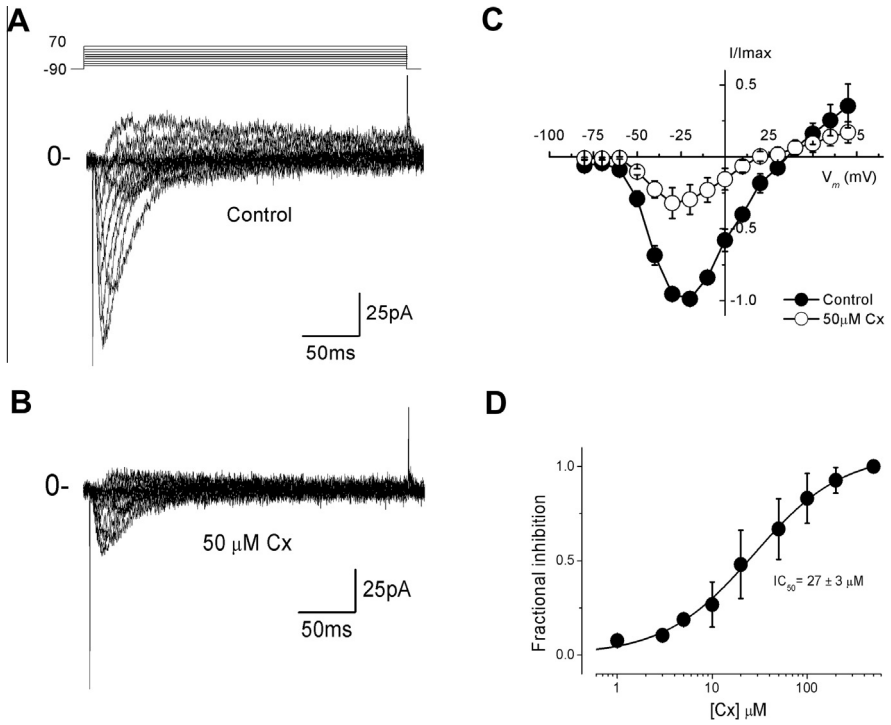

Fig. 1. Inhibition of T-type currents by Cx in mouse spermatogenic cells. (A) I_{Ca} evoked by depolarizing pulses from a −80 to + 70 mV applied in +10 mV increments under control conditions. (B) I_{Ca} recorded as in A but in the presence of 50 μM Cx. (C) Peak-current vs. voltage curve (*I–V*) constructed from traces as in A and B, as indicated. (D) Fractional I_{Ca} inhibition vs. [Cx]. Data points are (mean ± S.E.M., $n = 6$) of the fraction of blocked current at −20 mV for each Cx concentration. The line is the fit of the points with a Hill equation with $K_d = 27$ μM, and $n = 0.93$. HP = −90 mV.

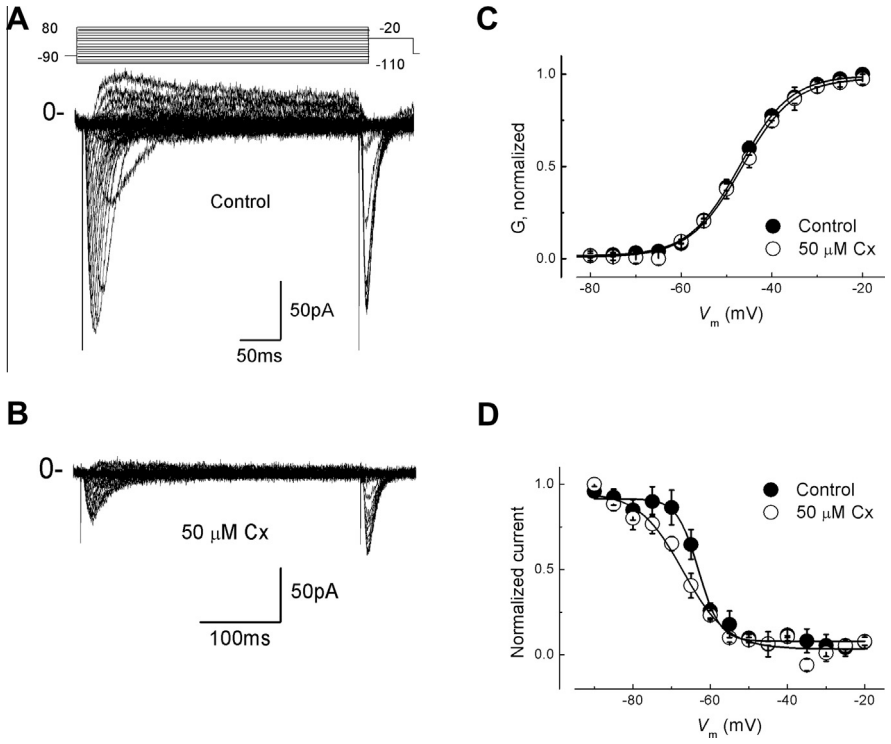

Fig. 2. Effect of Cx on the gating of T-type Ca^{2+} currents. (A) I_{Ca} recorded with the two-pulse protocol depicted at the top (see Text). (B) I_{Ca} recorded as in A but 50 μM Cx in the external solution. (C) Normalized Chord conductance (G) vs. V_m plot constructed in control (filled symbols) and in the presence of Cx (open symbols). The line is the fit of the points with the Boltzmann equation $G = 1/(1 + \exp((V_{50}\text{-}V_m)/k$. (D) Steady-state inactivation curves obtained from traces as in A and B, as indicated (see Text). The lines are least squares fits to a Boltzmann function $I_{Ca} = 1/(1 + \exp((V_{50}\text{-}V_m)/k)$. Bars represent S.E.M., $n = 6$.

the activation gating. In contrast, Cx has a significant effect on the steady-state inactivation curve. The points in Fig. 2D show that Cx shifts the inactivation curve to the left reducing its slope. This suggests that Cx facilitates channel inactivation in the range of voltages where channels dwell in intermediate closed states of the activation pathway (~−80 to −70 mV). The latter also indicates that at least part of the Cx inhibitory effect on T-type I_{Ca} is due to promotion of closed-state inactivation (see Section 4). Interestingly, and as mentioned above, the latter is accomplished with no evident modification of the open-state inactivation.

3.3. Cx stabilizes the inactivated state of T-type Ca^{2+} channels

Cx modification of inactivation was further characterized by assessing the stability of the inactivated state, measuring recovery from inactivation with a standard two pulse protocol, as illustrated in the left panel of Fig. 3A (0 Cx) and B (50 μM Cx). In the absence of Cx, recovery from inactivation develops in a single exponential phase (Fig. 3A right panel), with a time constant τ_h of 68 ± 3 ms, $n = 6$ at −100 mV (see figure legend). On the other hand, upon Cx addition, recovery from inactivation becomes drastically slower, indicating that the stability of the inactivated state is significantly increased (Fig. 3B; τ_h(Cx) = 385 ± 62 ms, $n = 6$). The above observations further demonstrate that Cx inhibits I_{Ca} at least partly by facilitating intermediate-closed state inactivation and by stabilization of the final inactivated state, thus significantly decreasing the channel's availability to conduct.

Regardless the detailed mechanism of Cx depression of T-currents, this effect may impair spermatogenic cell maturation and therefore fertilization. The role of Cx on the latter was further studied by assessing its effect on sperm cells.

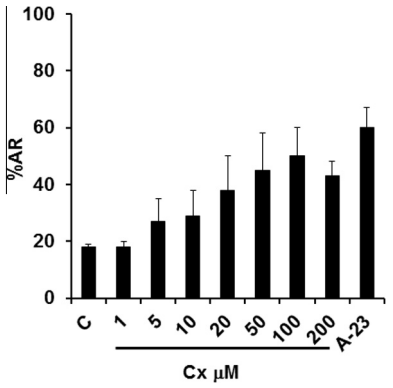

Fig. 4. Cx induces AR in mature sperm cells. Capacitated mouse sperm were exposed to increasing concentrations of Cx (1–200 μM). AR was quantified as a percentage relative to the maximal AR induced by the ionophore A23187 (see Section 2). Column labeled C indicates spontaneous AR. Bars represent SEM, $n = 3$ mice.

3.4. Cx triggers the acrosome reaction

Considering the role of Ca^{2+} on AR and the inhibitory effect of Cx on T-type Ca^{2+} channels, we anticipated that Cx would inhibit AR to reveal the involvement of T-type channels in this event. In order to test this hypothesis we determined the percentage of sperm that undergo AR when exposed to the range of [Cx] that inhibited T-type currents in spermatogenic cells (Fig. 4). The results in Fig. 4 show that instead of being inhibited, AR actually increased upon addition of Cx (~30% AR with 10 μM Cx vs. 20% spontaneous AR, $P < 0.05$). The last bar shows the standard positive control of AR

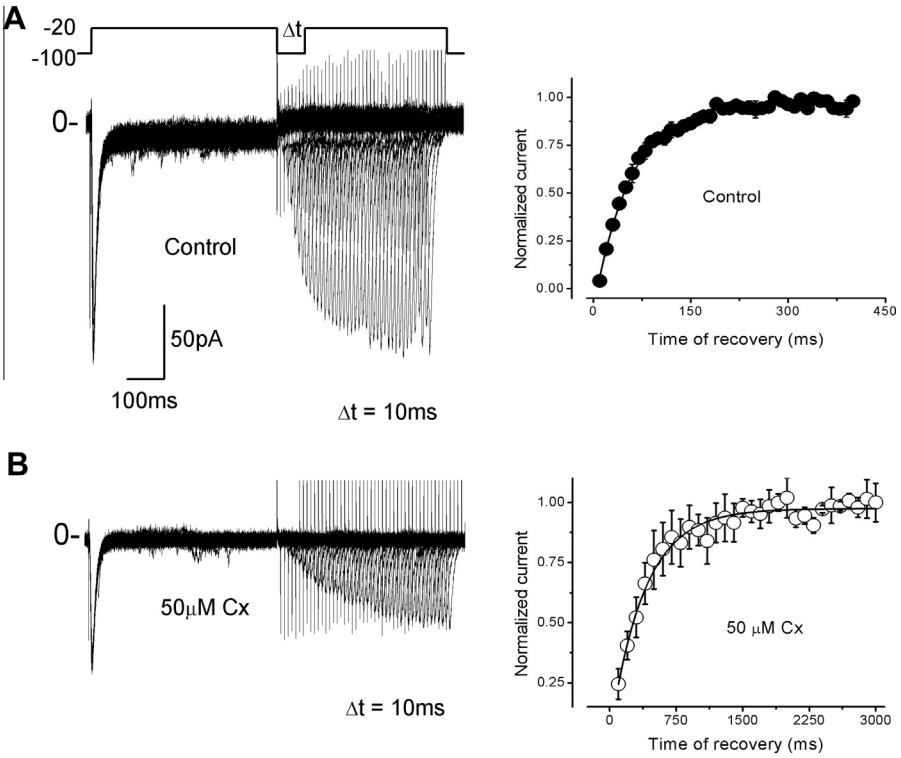

Fig. 3. Cx slows down recovery from inactivation. (A) Recovery from inactivation in control conditions. I_{Ca} recovery was evaluated by applying a 500 ms pulse to −20 mV that activates and inactivates channels. Thereafter the membrane was repolarized to the HP of −100 mV for the indicated time interval. Finally, recovery was tested applying a −20 mV pulse. Left panel, representative control I_{Ca}. Right panel, extent of recovery obtained from traces as in the left panel (B). Recovery from inactivation in the presence of 50 μM Cx. Time course of recovery was fitted with a single exponential equation (solid lines through the points) with time constants τ_h of 68 ms for control and 385 ms in the presence of 50 μM of Cx. Error bars represent SEM ($n = 6$).

(~70% AR upon addition of the Ca^{2+} ionophore A-23187). These findings demonstrate that, unexpectedly, Cx triggers AR in mature mouse sperm (see Section 4).

Taking into account the above puzzling effect on AR, a process that necessarily requires an elevation intracellular Ca^{2+} to occur, we sought to determine the $[Ca^{2+}]_i$ of mature sperm upon Cx addition.

3.5. Cx elevates $[Ca^{2+}]_i$ in mature sperm

$[Ca^{2+}]_i$ changes promoted by Cx addition were determined by loading mouse sperm with the fluorescent dye Fluo-4 (see Section 2). Fig. 5A–C shows image sequences of Fluo-4 loaded sperm bathed in a medium containing 2 mM $[Ca^{2+}]_{ext}$ before and after the addition of 50 μM Cx, as indicated (see figure legend). Note that

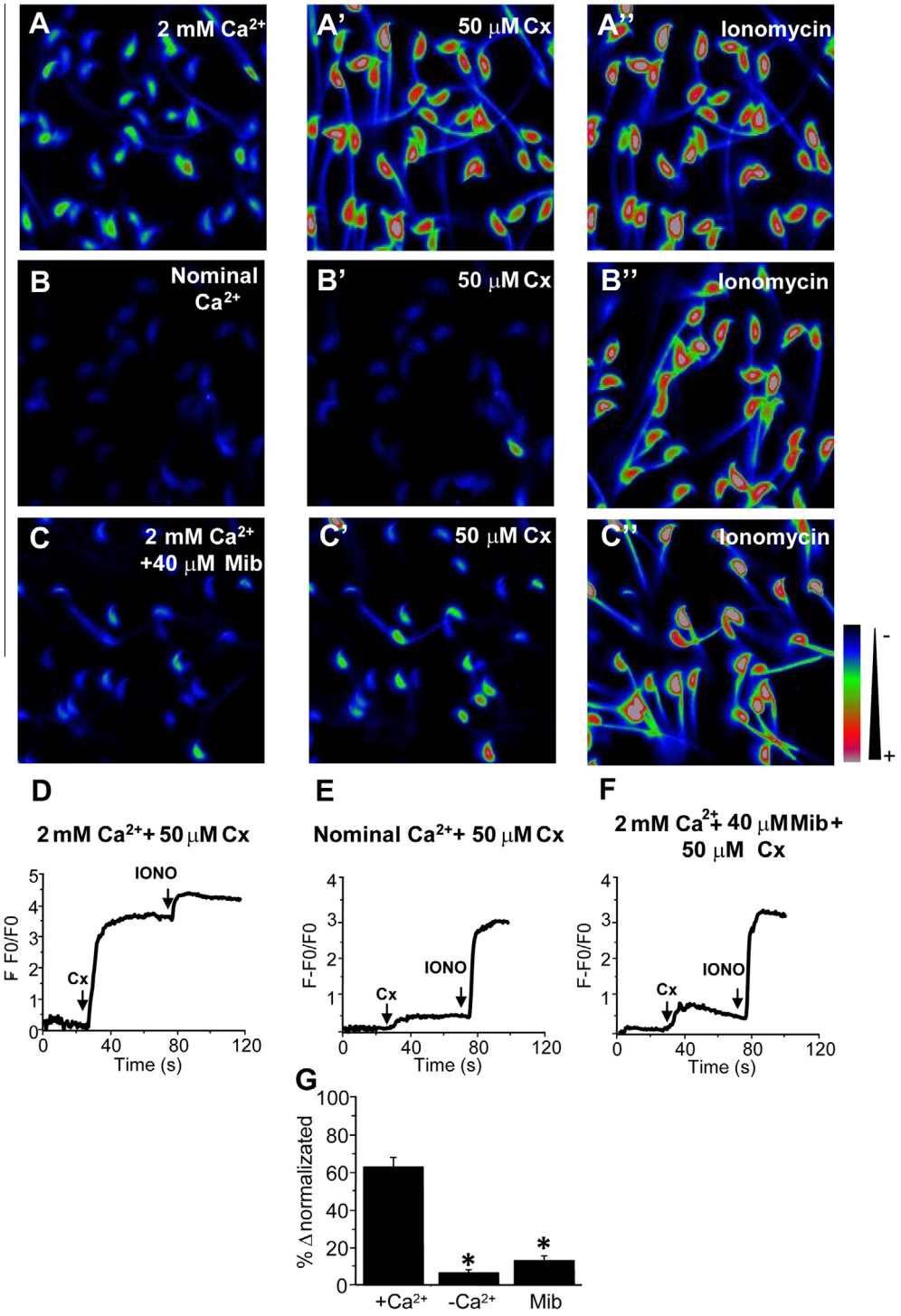

Fig. 5. The Cx induced increase in $[Ca^{2+}]_i$ depends on the presence of external Ca^{2+}. Pseudo-colored fluorescence images obtained by loading sperm with Fluo-4 (see Section 2). Upper panel, (A) fluorescence signal with 2 mM Ca^{2+} in the recording chamber; (A′) $[Ca^{2+}]_i$ increase after the addition of 50 μM Cx; (A″) $Ca^{2+}{}_i$ increase after adding 10 μM ionomycin. Middle panel, (B) fluorescence signal in the presence of nominal 0 Ca^{2+} in the recording chamber; (B′) 0 Ca^{2+} plus 50 μM Cx; (B″) ionomycin plus 2 mM Ca^{2+}. Lower panel, (C) fluorescence signal with 2 mM Ca^{2+} and 40 μM mibefradil in the recording chamber; (C′) as in C but with 50 μM Cx; (C″) ionomycin. (D–F) $F - F_0/F_0$ traces showing the increments in $[Ca^{2+}]_i$ under the conditions indicated above. (G) Percent of Δ-fluorescence increase normalized to the ionomycin response in 2 mM $[Ca^{2+}]_o$ (+Ca^{2+}) (n = 66 cells), non-Ca^{2+} added (-Ca^{2+}) (n = 52 cells), and mibefradil (Mib) (n = 54 cells), $^*P < 0.001$) n = 5 mice.

Cx clearly increased $[Ca^{2+}]_i$ (Fig. 5A–A″ and D). In the Figure, 10 μM ionomycin containing 2 mM Ca^{2+} was added to calibrate the fluorescent changes promoted by Cx to the maximum response elicited by the ionophore, which in addition is a positive control of cell viability (Fig. 5A″–C″). Interestingly, the $[Ca^{2+}]_i$ increases induced by Cx depend on extracellular Ca^{2+}. This is seen in Fig. 5B–B″ and Fig. 5E, which show that the Cx response in an external media nominally lacking Ca^{2+} was drastically reduced (Fig. 5B′). The latter also shows that even though Cx is a lipid soluble molecule it does not affect sperm intracellular Ca^{2+} stores.

Finally, in order to gain some insight regarding the Cx molecular target(s) underlying the increase of $[Ca^{2+}]_i$ (Fig. 5A–A″) we added Cx in the presence of mibefradil, a compound that inhibits the sperm-specific CatSper Ca^{2+}-channel [11]. The results in Fig. 5C–C″and F show that mibefradil greatly reduced the Cx-promoted increase of $[Ca^{2+}]_i$. The above observations are summarized in Fig. 5G which compares the normalized fluorescent changes observed upon Cx addition in the three conditions tested.

Our findings indicate that despite of its inhibition of T-type channels, Cx nevertheless stimulates increases in $[Ca^{2+}]_i$. This may occur by up-regulating CatSper channels, as suggested by the effect of mibefradil. Considering that CatSper is activated by both alkalinization and membrane depolarization we assessed the effect of Cx on these two parameters.

3.6. Cx elevates pH_i and depolarizes the plasma membrane of mature sperm

Spermatozoa loaded with the pH-sensitive dye BCECF (see Methods) underwent a Cx induced increase in pH_i. Fig. 6A shows that this increases can be detected starting at [Cx] $\geqslant$30 μM and reaches a maximum at ~90 μM (~0.3 units; Fig. 6B and Supplementary Fig. 3). These results are consistent with the possibility that Cx may activate ion channels sensitive to pH_i such as CatSper and SLO3. The activation of CatSper would result in $[Ca^{2+}]_i$ increase and promotion of AR. Activation of a Ca^{2+} channel or inhibition of a K^+ channel would cause a depolarization. Therefore, the effect of Cx on membrane potential was assessed using the voltage-sensitive dye DisC3. Fig. 6C shows that 20–50 μM Cx depolarizes non-capacitated sperm by ~20 mV. This finding is consistent with the Cx induced stimulation of a Ca^{2+} conductance (Fig. 5) sensitive to pH_i but does not discard the possibility that the inhibition of a K^+ conductance by Cx could contribute to membrane depolarization. Further studies are needed to test this hypothesis.

4. Discussion

In this study we have shown that the NSAID celecoxib inhibits T-type Ca^{2+} channels in mouse spermatogenic cells and affects the Ca^{2+}, pH_i and membrane potential homeostasis of sperm. All things considered, Cx may hinder fertilization.

4.1. Cx inhibition of T-type I_{Ca} in spermatogenic cells

It has been shown that Cx inhibits L-type I_{Ca} [41]. We observed that T-type Ca^{2+} channels of spermatogenic cells are also inhibited by Cx added to the external solution, with a K_d of 27 μM. The dose–response curve indicates that Cx binds to the channels with 1:1 stoichiometry, suggesting that the protein presents a single site where this drug is able to bind at low micromolar concentrations similar to those found in human plasma (5–15 μM) [31], inhibiting I_{Ca}.

T-type channels inactivate from both open and closed states [8,32,35]. In contrast to its lack of effect on open-state inactivation, here we have shown that Cx increases the fraction of channels that inactivate at intermediate negative potentials where channels dwell in intermediate closed states of the activation pathway, thus changing the slope of the steady-state inactivation curve, shifting the V_{50} to the left, and decreasing channel availability.

The I_{Ca} inhibition exerted by the Cx-enhanced closed-state inactivation is reinforced by the drastic decrease that the drug produces in the rate of recovery from inactivation. Notably, hyperpolarization does not diminish this effect. This is in contrast with observations on K^+ channels of the Shab family in which Cx also slows recovery from inactivation but the effect is relieved by membrane hyperpolarization [1]. This difference could possibly arise from the characteristic lack of voltage dependence of recovery from inactivation of T-type Ca^{2+} channels at hyperpolarized voltages [35].

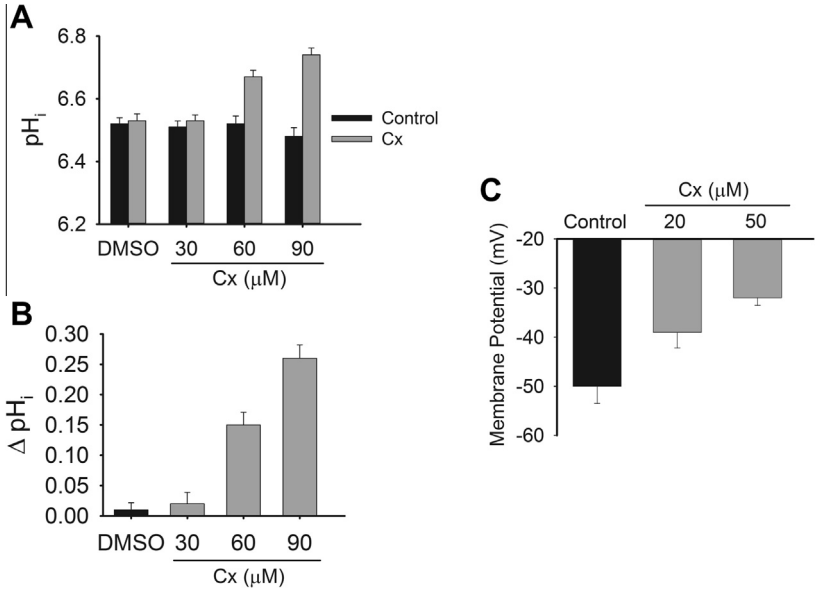

Fig. 6. Cx increases pH_i in mature mouse sperm and depolarizes the membrane. pH_i was measured using BCECF (0.5 μM) as described in Section 2. (A) pH_i before (black bars) and after (gray bars) Cx addition. (B) Incremental pH_i change (ΔpH_i) caused by the indicated [Cx]. DMSO was used as a control. ** $P \leqslant 0.01$ (n = 4). (C) V_m values (see Section 2) as a function of [Cx]. V_m under control conditions (~-50 mV) was depolarized ~ + 20 mV in the presence of 50 μM Cx. Bars represent SEM, n = 3.

4.2. Cx increase of $[Ca^{2+}]_i$ and AR induction

Considering that mammalian AR requires Ca^{2+} uptake and T-type Ca^{2+} channels have been implicated in this process [2,20], we expected Cx to inhibit the mouse AR. Unexpectedly our findings showed that Cx triggered this Ca^{2+}-dependent process at concentrations that inhibited T-type channels in spermatogenic cells (Fig. 4), an apparent paradox that we investigated further. It is important to note that a low but significant AR induction was provoked by Cx at concentrations as low as 5 μM, which are in the range of those reported in human plasma [31]. As the AR is a process highly dependent on extracellular Ca^{2+} and our results show a clear inhibitory effect of T-type channels by Cx when studied in spermatocytes, we believe that another Ca^{2+} entry mechanism is being activated by this drug when studied in mature spermatozoa. One of the major candidates to contribute to this Ca^{2+} uptake is the CatSper channel, which has been shown to be a promiscuous ion channel [5]. Although it is not clear if Cx could directly activate CatSper or indirectly by rising intracellular pH, our study suggests that an additional Ca^{2+} conductance other than T-type channels may participate in AR.

Consistent with its effect on AR, we found that Cx increases $[Ca^{2+}]_i$ and pH_i, and depolarizes non-capacitated sperm. We consider that, besides the chemical nature of Cx as an amide [10,17], this compound may cause an alkalization by inhibiting carbonic anhydrases present sperm cells [24,29,38]. Alkalization may in turn activate two major and well documented participants in the mammalian AR, CatSper Ca^{2+} and SLO3 K^+ channels [11,19,22]. The pH-mediated activation of SLO3 should hinder the observed membrane depolarization, as it would do the Ca^{2+}-dependent activation of SLO1 K^+ channels [11]. Taking this into account we cannot discard the possibility that Cx might inhibit SLO channels, an effect that has been observed on other K^+ channels [13,14]. On the other hand, Ca^{2+} entry through the alkalization-activated CatSper would depolarize the membrane and elevate $[Ca^{2+}]_i$, promoting AR. This contention is supported by the fact that the Cx induced $[Ca^{2+}]_i$ increase is sensitive to mibefradil, a CatSper blocker. Although further work is needed to test this proposal, our observations unmistakably demonstrate that the broadly commercialized and commonly used NSAID Cx compromises critical steps of the fecundation process.

Acknowledgements

We thank Dr. Chris Wood for comments on the manuscript and Yoloxochitl Sanchez and Dr. Gerardo Orta for technical assistance during the development of this work. This work was supported by Consejo Nacional de Ciencia y Tecnología (CONACyT) Grant 128566, by the National Institutes of Health (NIH), grant P-304 to Pablo Visconti and by DGAPA-UNAM IN211809-3 (to Dr. Alberto Darszon) and by Dirección General de Asuntos del Personal Académico/Universidad Nacional Autónoma de México (IN202212-3 to CT).

Appendix A. Supplementary data

Supplementary data associated with this article can be found, in the online version, at http://dx.doi.org/10.1016/j.febslet.2013.05.068.

References

[1] Arias-Olguín, I.I., Carrillo, E., Meza-Torres, B., Barriga-Montoya, C., Balleza, D. and Gómez-Lagunas, F. (2011) Induction of a fast inactivation gating on delayed rectifier Shab K(+) channels by the anti-inflammatory drug Celecoxib. Channels 1, 56–64.
[2] Arnoult, C., Cardullo, R.A., Lemos, J.R. and Florman, H.M. (1996) Activation of mouse sperm T-type Ca^{2+} channels by adhesion to the egg zona pellucid. Proc. Natl. Acad. Sci. USA 93, 13004–13009.
[3] Arnoult, C., Villaz, M. and Florman, H. (1998) Pharmacological properties of the T-type Ca^{2+} current of mouse spermatogenic cells. Mol. Pharmacol. 53, 1104–1111.
[4] Balderas, E., Arteaga-Tecuitl, R., Rivera, M., Gomora, J.C. and Darszon, A. (2012) Niflumic acid blocks native and recombinant T-type channels. J. Cell. Physiol. 227 (6), 2542–2555.
[5] Brenker, C., Goodwin, N., Weyand, I., Kashikar, N.D., Naruse, M., Krähling, M., Müller, A., Kaupp, U.B. and Strünker, T. (2012) The CatSper channel: a polymodal chemosensor in human sperm. EMBO J. 31 (7), 1654–1665.
[6] Brueggemann, L.I., Mackie, A.R., Mani, B.K., Cribbs, L.L. and Byron, K.L. (2009) Differential effects of cyclooxygenase-2 inhibitors on vascular smooth muscle ion channels may account for differences in cardiovascular risk profiles. Mol. Pharmacol. 76 (5), 1053–1061.
[7] Carlson, A.E., Westenbroek, R.E., Quill, T., Ren, D., Clapham, D.E., Hille, B., Garbers, D.L. and Babcok, D.F. (2003) CatSper 1 required for evoked Ca^{2+} entry and control of flagellar function in sperm. Proc. Natl. Acad. Sci. USA 100, 14864–14868.
[8] Catterall, W.A. (2000) Structure and regulation of voltage-gated Ca^{2+} channels. Annu. Rev. Cell Dev. Biol. 16, 521–555.
[9] Chavez, J.C., Hernandez-Gonzalez, E.O., Wertheimer, E., Visconti, P.E., Darszon, A. and Trevino, C. (2012) Participation of the Cl^-/HCO_3^- exchangers SLC26A3 and SLC26A6, the Cl^- channel CFTR and the regulatory factor SLC9A3R1 in mouse sperm capacitation. Biol. Reprod. 86 (1), 1–14.
[10] Cierpicki, T. and Otlewiski, J. (2001) Amide proton temperature coefficients as hydrogen bond indicator in proteins. J. Biomol. NMR 21, 249–261.
[11] Darszon, A., Nishigaki, T., Beltran, C. and Trevino, C.L. (2011) Calcium channels in the development, maturation and function of spermatozoa. Physiol. Rev. 91 (4), 1305–1355.
[12] Fraire-Zamora, J.J. and González-Martínez, M.T. (2004) Effect of intracelular pH on depolarization-evoked calcium influx in human sperm. Am. J. Cell Phys. 287, 1688–1696.
[13] Frolov, R.V., Slaughter, M.M. and Singh, S. (2008) Effect of celecoxib on ionic currents and spontaneous firing in rat retinal neurons. Neuroscience 154 (4), 1525–1532.
[14] Frolov, R.V., Bondarenko, V.E. and Singh (2010) Mechanism of KV2.1 channel inhibition by celecoxib-modification of gating and channel block. Br. J. Pharmacol. 159, 405–418.
[15] Hagiwara, S. and Kawa, K. (1984) Calcium and potassium currents in spermatogenic cells dissociated from rat seminiferous tubules. J. Physiol. 356, 135–149.
[16] Henkel, R.R. and Schill, W.B. (2003) Sperm preparation for ART. Reprod. Biol. Endocrinol. 14, 1–108.
[17] Homer, R.B. and Johnson, C.D. (1970) in: The Chemistry of Amides (Zabicky, J., Ed.), Wiley, New York. Chapter 3.
[18] Kirichok, Y., Navarro, B. and Clapham, D.E. (2006) Whole-cell patch-clamp measurements of spermatozoa reveal an alkaline-activated Ca^{2+} channel. Nature 439, 737–740.
[19] Leonetti, M., Yuan, P., Hsiung, Y. and MacKinnon, R. (2012) Functional and structural analysis of the human SLO3 pH- and voltage-gated K+ channel. Proc Natl Acad Sci. 109, 19274–19279.
[20] Liévano, A., Santi, C.M., Serrano, C.J., Treviño, C.L., Bellve, A.R., Hernández-Cruz, A. and Darszon, A. (1996) T-type Ca^{2+} channels and alpha 1E expression in spermatogenic cells, and their possible relevance to the sperm acrosome reaction. FEBS Lett. 388, 150–154.
[21] Lishko, P.V., Botchkina, I.L. and Kirichok, Y. (2011) Progesterone activates the principal Ca^{2+} channel of human sperm. Nature 471, 381–387.
[22] Lishko, P.V., Kirichok, Y., Ren, D., Navarro, B., Chung, J.J. and Clapham, D.E. (2012) The control of male fertility by spermatozoa ion channels. Annu. Rev. Physiol. 74, 453–475.
[23] Macías, A., Moreno, C., Moral-Sanz, J., Cogolludo, A., David, M., Alemanni, M., Pérez-Viscaíno, F., Zaza, A., Valenzuela, C. and González, T. (2010) Celecoxib blocks cardiac Kv1.5, Kv4.3 and Kv7.1 (KCNQ1) channels: effects on cardiac action potentials. J. Mol. Cell. Cardiol. 49 (6), 984–992.
[24] Marini, A.M., Maresca, A., Aggarwal, M., Orlandini, E., Nencetti, S., et al. (2012) Tricyclic sulfonamides incorporating benzothiopyrano [4,3-*c*]pyrazole and pyridothiopyrano[4,3-*c*]pyrazole effectively inhibit α- and β-carbonic anhydrase: X-ray crystallography and solution investigations on 15 isoforms. J. Med. Chem. 55 (22), 9619–9629.
[25] Martínez-López, P., Santi, C.M., Trevino, C.L., Ocampo-Gutiérrez, A.Y., Acevedo, J.J., Alisio, A., Salkoff, L.B. and Darszon, A. (2009) Mouse sperm K+ currents stimulated by pH and cAMP possibly coded by Slo3 channels. Biochem. Biophys. Res. Commun. 381 (2), 204–209.
[26] Muñoz-Garay, C., De la Vega-Beltran, J.L., Delgado, R., Labarca, P., Felix, R. and Darszon, A. (2001) Inwardly rectifying K(+) channels in spermatogenic cells: functional expression and implication in sperm capacitation. Dev. Biol. 234, 261–274.
[27] Navarro, B., Kirichok, Y. and Clapham, D. (2007) Ksper, a pH sensitive K+ current that controls sperm membrane potential. Proc. Natl. Acad. Sci. 104 (18), 7688–7692.
[28] Nishigaki, T., Wood, C.D., Tatsu, Y., Yumoto, N., Furuta, T., Elias, D., Shiba, K., Baba, S.A. and Darszon, A. (2004) A sea urchin egg jelly peptide induces a cGMP-mediated decrease in sperm intracellular Ca(2+) before its increase. Dev. Biol. 272 (2), 376–388.

[29] Pakkila, S., Kaunisto, K., Kellokumpu, S. and Rajaniemi, H. (1991) A high activity carbonic anhydrase isoenzyme (CaII) is present in mammalian spermatozoa. Histochemistry 95, 477–482.
[30] Park, S.Y., Kim, T.H., Kim, H.I., Shin, Y.K., Lee, C.S., Park, M. and Song, J.H. (2007) Celecoxibe inhibits Na+ currents in rat dorsal root ganglion neurons. Brain Res. 1148, 53–61.
[31] Park, M.S., Shim, W.S., Yim, S.V. and Lee, K.T. (2012) Development a simple and rapid LC–MS/MS method for determination of celecoxib in human plasma and its application to bioequivalence study. J. Chromatogr., B 902, 137–141.
[32] Perez-Reyes, E. (2003) Molecular physiology of low-voltage-activated T-type calcium channels. Physiol. Rev. 83, 117–161.
[33] Quill, T.A., Ren, D., Clapham, D.E. and Garbers, D.L. (2001) A voltage-gated ion channel expressed specifically in spermatozoa. Proc. Natl. Acad. Sci. USA 22, 12527–12531.
[34] Santi, C.M., Darszon, A. and Hernández-Cruz, A. (1996) A dihydropyridine-sensitive T-type Ca^{2+} current is the main Ca^{2+} current carrier in mouse primary spermatocytes. Am. J. Physiol. 271, 1583–1593.
[35] Serrano, J.R., Perez-Reyes, E. and Jones, S.W. (1999) State-dependent inactivation of the alpha 1G T-type calcium channel. J. Gen. Physiol. 114 (2), 185–201.
[36] Sheng, H., Shao, J., Kirkland, S.C., Isakson, P., Coffey, R.J., Morrow, J., Beauchamp, R.D. and DuBois, R.N. (1997) Inhibition of human colon cancer cell growth by selective inhibition of cyclooxygenase-2. J. Clin. Invest. 99 (9), 2254–2259.
[37] Strunker, T., Goodwin, N., Brenker, C., Kashikar, N.D., Weyand, I., Seifert, R. and Kaupp, U.B. (2011) The CatSper channel mediates progesterone-induced Ca^{2+} influx in human sperm. Nature 471, 382–386.
[38] Weber, A., Casini, A., Heine, A., Kunh, D., Claudiu, T., Scozzafava, A. and Klebe, G. (2004) Unexpected nanomolar inhibition of carbonic anhydrase by COX-2-selective celecoxib: new pharmacologycal opportunities due to related binding site recognition. J. Med. Chem. 47, 550–557.
[39] Xia, J., Reigada, D., Mitchell, C.H. and Ren, D. (2007) CATSPER channel-mediate Ca^{2+} entry into mouse sperm triggers a tail-to-head propagation. Biol. Reprod. 77, 551–559.
[40] Xia, J. and Ren, D. (2009) The BSA-induced Ca^{2+} influx during sperm capacitation is CATSPER channel-dependent. Reprod. Biol. Endocr. 7, 119.
[41] Zhang, Y., Tao, J., Huang, H., Ding, G., Cheng, Y. and Sun, W. (2007) Effects of celecoxib on voltage-activated calcium channel current in rat pheocromocytoma (PC12) cells. Pharmacol. Res. 57, 267–274.
[42] Zhang, X., Zeng, X. and Lingle, C. (2006) Slo3 K+ channel: voltage and pH dependence of macroscopic currents. J. Gen. Physiol. 128 (3), 317–336.
[43] Zeng, X., Yang, C., Kim, S., Lingle, C. and Xia, X. (2011) Deletion of the Slo3 gene abolishes alkalinization-activated K+ current in mouse spermatozoa. Proc. Natl. Acad. Sci. 108 (14), 5879–5884.